3.4.4. Scientific data processing

The SDPSW is the component handling the processing of data collected by the SWA-EAS (1 and 2) and SWA-PAS sensors, while SWA-HIS processes scientific data on its own. Due to the limited bandwidth available to SWA for downlink, the full set of SWA raw data collected cannot be transmitted back to ground at all times. Indeed, even to return full resolution data products at relatively low time cadences requires compression rates (CR) in the range from 2 to 7.6, depending on the different kinds of data and their associated data product volumes. In order to return information on the nature of the solar wind at higher cadences, data processing within the SWA-DPU is used to evaluate derived scientific properties of the solar wind, in particular the moments of the particle VDF (Paschmann et al. 1998). These quantities are transmitted instead of the full raw data, with the transmission of full VDFs only at lower cadence or after appropriate compression. The processing of SWA-EAS1, SWA-EAS2, and SWA-PAS scientific data generated during their normal and burst modes is handled by the PCMSW that calls the services offered by the SDPSW, within its cyclic activities routine. Accordingly, the execution of scientific algorithm requests, such as "Compress Data Product" or "Calculate Moments", is distributed across several different run-time intervals. This is managed by means of dedicated activity tables defining the actions the SDPSW has to perform for each "activation" by the PCMSW. These tables define the software behaviour for both compression and moment calculation functions for each sensor and for each operating mode, according to the specific data collection rate and order. In this way, the SDPSW prepares data as they are ingested by the SWA-DPU from sensors, and, when the complete data sample to be processed has been reconstructed, the SDPSW's services start data compression (or moments calculation) and continue, with cyclic activation, until that operation is completed.

On board moments calculation. The SDPSW provides the functionality for the calculation of the number density (moment of order zero), number flux density (first order moment), pressure tensor (second order moment: computed in the satellite reference frame for SWA-EAS and SWA-PAS), and energy flux density vector (third order moment: computed only for SWA-EAS). Moments are computed starting from the counts accumulated in each elementary volume in phase space and with reference to the sensor' resolution in energy, azimuth, and elevation angles (Paschmann et al. 1998). From an operational point of view, all the equations defining the moments have been captured within a series of LUTs allowing the performance of the moments calculation by means of only sums and products, with the counts of each elementary volume in phase space "modulated" by a combination of these factors. This algorithm has an initialisation phase that is performed only at SWA-DPU start-up and must be repeated each time the configuration values are updated from ground. It is a deterministic set of computations, and can be completely verified on-ground. Algorithm configuration values are read from memory (MRAM) and used to evaluate a set of "constant" parameters used as LUTs at run-time. Some of these tables contain configuration parameters derived on the ground from the sensor physical and geometrical properties. Others parameters which are expected to show slow time variation are held in LUTs which can be readily updated from the ground. For some parameters, particularly those which are directly linked with the way sensors are commanded to sweep energies or elevations, the same inputs are shared for both sensor and SDPSW configurations. For example, both the SWA-EAS-Sequencer and the SWA-DPU-SDPSW rely on the same ground commandable parameters defining the hemisphere voltage ratio and maximum voltage. The output is the same hemisphere LUT composed of 64 values expressed in volts and eV. Other commandable LUT parameters include those fixing the range of variability and the precision at which a given set of moments will be telemetered to ground; this is done by defining the couplet of information (LSB, Offset) to be applied to the raw and scientific data in order to define the transmitted value within the data packet.

The calculation of accurate moments from the SWA-EAS sensor is dependent on identifying and removing data from those low energy bins which may be contaminated by the presence of spacecraft photo-electrons. Since such electrons are generally found at energies below the spacecraft potential, the baseline algorithm involves the use of a measurement of that potential passed to the SWA-DPU from the RPW experiment (Maksimovic et al. 2020), if it proves reliable, or otherwise using a fixed but ground-commandable level. This information is transmitted via the Service 20 IEL. The moment calculation then does not include SWA-EAS1 and SWA-EAS2 energy bins with ranges which are partially or fully below the value of the spacecraft potential. Moreover, the ranges of the energy bins above the spacecraft potential are reduced by the value of the spacecraft potential. In addition, moments are calculated as partial summations across three energy ranges (see Sect. 4.3 for details), so that even if the lower range is contaminated, some useful science data will remain in the upper ranges.

Data compression. Representative sample data have been produced by extrapolating real measurements by the Cluster mission to the conditions in which SWA is expected to operate. These have been evaluated for their information content, using both the data entropy measure and the actual CR. Results from this exercise demonstrate that SWA-EAS data CR can vary between ~1.9 and ~12.1, while for SWA-PAS data this ranges from ~3.4 to ~17.5. Data compression is performed by means of a customised implementation of the lossless Consultative Committee for Space Data Systems (CCSDS) 121.0 standard. This choice has been made as a trade-off between compression and computational efficiency. In fact, the CCSDS 121 technique allows full exploitation of the intrinsic structure exhibited by all data products, together with information theory methods, while remaining within the computational resource limitations. In particular, a specific customisation was designed for SWA-EAS data in order to reach the compression ratio needed, by detailed consideration of the specific data structure. SWA-EAS samples produce 3-dimensional matrices (cubes) whose dimensions cover the elevation and azimuth of incoming particle directions and their energy levels. These cubes are stored in a rolling buffer, within the SWA-DPU's memory, in a specifically defined one-dimensional array, mostly dependent on the acquisition sequence (simply meaning the first sample acquired is the first in the array). However, a preferential scanning sequence, which is different to that of the actual acquisition, has been identified from simulations using existing solar wind data. This sequence is identified by measuring similarities in each direction within the 3D data in order to identify which demonstrates the slowest variation rate. Thus, a further processing step is preliminarily applied to sampled SWA-EAS electron distributions in order to increase the algorithm's performance in terms of better prediction efficiencies, smaller prediction errors, and ultimately higher achievable compression ratio. This "complex reordering" mechanism has thus been designed in order to exploit the preferential direction in data similarity. It switches the data order

after acquisition (this mechanism is identified as the "simple" reordering step), and then ensures that the highest degree of spatial continuity is established between contiguous samples (this mechanism is identified as the "complex" reordering step).

For SWA-EAS data, it has been found that a simple reordering of the data from the original order, that is elevation angle, energy level, azimuthal angle to energy level, azimuthal angle, elevation angle, brings clear improvements in the compression efficiency. In addition, the complex reordering step further improves compression performances by avoiding periodic jumps between acquisition directions. Re-ordered data are then passed to the unit-delay predictor and the standard pre-processing module. In the final compression step, the coder applies Rice's technique, in which several algorithms are concurrently applied to a block of consecutive pre-processed samples. The algorithmic option that yields the shortest encoded length for the current block of data are selected for transmission.

Book-keeping algorithm (BKA). The SWA-DPU ASW is responsible for controlling data collection, mode use, and imposing telemetry generation restrictions on each of the three SWA sensors separately, in order to keep each of them within the respective assigned allocations. In principle, during burst modes the sensors generate raw data at a rate which is significantly higher than their orbit-averaged allocation, while in normal mode they generate data products at a slightly slower rate than is consistent with the orbit allocation for each sensor. Thus, the book-keeping algorithm (BKA) is a software tool able to monitor and control the amount of burst mode used against the pro-rata expectation for any given point along the orbit. The principles underpinning the BKA are:

1. The BKA will be used by the ASW to assess the generation rate of science data by each of the three SWA sensors over an established time interval that starts at time T_0 and ends at time $T_0 + \Delta T$. ΔT is variable to allow for lessons learnt in flight, but the initial baseline should be the orbital period of the spacecraft or duration of a stable telemetry corridor (Sanchez et al., in prep.);

2. The ASW will hold record of two limits per sensor, set by the SWA team (changeable in flight to account for lessons learnt) representing: (a) the fractional level, O_S, against which the sensors may be allowed to become overdrawn against the pro-rata allocation, and; (b) the fractional level, U_S, against which an unacceptable "under-drawing" against the pro-rata allocation is deemed to have occurred;

3. At regular intervals the ASW will update the accumulated total volume, $V_{BM,S}(t)$, of post-processed data which has been originated by sensor S since time T_0.

4. At regular intervals, the ASW will calculate $A_{BM,S}(t)$, the expected pro-rata data accumulation for each sensor, S, since time T_0, based on the orbit-averaged allocation, $A_{BM0,S}$, for that sensor:

$$A_{BM,S}(t) = A_{BM0,S} \times \frac{(t - T_0)}{\Delta T} \tag{1}$$

5. The ASW will ensure that each sensor, S, does not produce so much BM data that the difference between the actual accumulated total volume, $V_{BM,S}(t)$, of data from sensor S which has been sent to the spacecraft solid state mass memory (SSMM) since time T_0, and the pro-rata orbit allocation $A_{BM,S}(t)$ does not exceed the fraction O_S of the remaining allocation. If the fraction is exceeded, then the SWA-DPU will disable trigger event capture and disable further optional scheduled burst modes until the excess is reduced to a factor of, at most, $M \times O_S$. Specifically, the SWA-DPU will disable optional scheduled BM and trigger event capture if:

$$V_{BM,S}(t) > A_{BM0,S} \times \left[\frac{(1 - O_S)(t - T_0)}{\Delta T} + O_S \right] \tag{2}$$

and will subsequently re-enable schedule BM and trigger event capture once:

$$V_{BM,S}(t) < A_{BM0,S} \times \left[\frac{(1 - MO_S)(t - T_0)}{\Delta T} + MO_S \right] \tag{3}$$

6. In a similar way the SWA-DPU will ensure that $V_{BM,S}(t)$ does not fall below the fraction U_S of the remaining allocation. If the fraction is not achieved, then the SWA-DPU will enable additional scheduled burst modes until the underspend is reduced to a factor of less than $M \times U_S$ enabling additional scheduled BM;

7. In any case, the assessment period can be restarted once the period ΔT has elapsed. At this time, the accumulated data should have only a relatively small difference from the maximum allowed total for the orbit or period. Thus the assessment can be restarted by carrying over the small difference to the next assessment period;

8. The BKA is also able to handle ground commands for the ASW operation, which set the trigger-enable flag and control the amount of scheduled burst mode for limited specific periods, and automatically recover the required average telemetry rate in the following period;

9. All the parameters controlling the operation of the BKA are configurable in flight to allow the ASW to control the data production when the available telemetry rate is reduced below the nominal level. In practice this is likely to require (temporary) changes to the parameters O_S, U_S, and $A_{BM0,S}$ by ground command for the duration of such periods, with possible compensatory changes to allow catch-up outside these periods;

10. The ASW is able to restart the BKA and resume correct operation in the event of a reboot or restart of the SWA-DPU.

The requirement to steer the SWA data accumulation through a telemetry corridor (defined for any given period at mission level) is equivalent to choosing a particular set of the BKA configuration parameters defined above. This will allow the SWA BKA to control SWA telemetry generation to remain within a defined telemetry corridor. This is illustrated in Fig. 30.

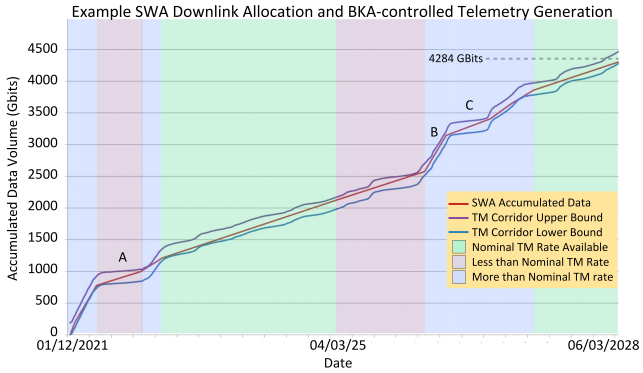

Fig. 30. Operation of the SWA BKA. Mission periods occur when less than (pink shading), more than (blue), and actual (green) nominal data rates will be available. The SWA BKA will steer data production (red line) through a project defined telemetry corridor with upper and lower limits (purple and blue lines respectively). Periods of low download rates (e.g. marked A and C) can be optimally negotiated by the BKA using higher rates on ether side (e.g. at point B).

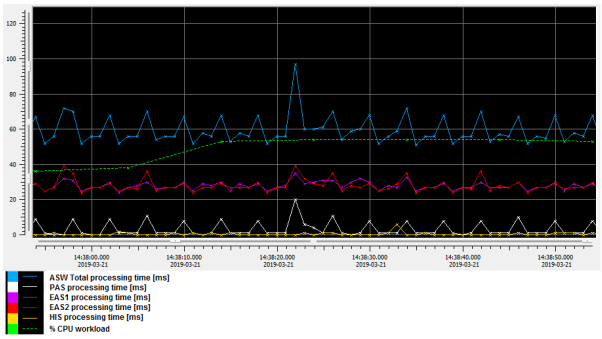

Fig. 31. Illustration of SWA-DPU performance. DPU activity enhancements associated with the 4 s cadences of SWA-EAS and SWA-PAS in normal mode are clearly visible.

3.4.5. SWA-DPU testing and characterisation

Figure 31 shows the ASW performance in the worst case condition occurring in periods in which all sensor scientific activities are activated, the compression algorithm is enabled, and a freeze of the trigger mode rolling buffer has been activated following the simulated receipt of a flag from the RPW instrument (Maksimovic et al. 2020) via PUS Service 20. Even under these conditions, the ASW performance remains under the required limit. In particular, we note that during each ASW processing slot (ASW activity cycles at 8 Hz) the ASW total processing time is lower than the maximum allowed time of 125 ms with the maximum time measured being 97 ms. In addition, the SWA-EAS and SWA-PAS processing times are largely uniform during science processing, and peaks are due to moment computation performed each 4 s and full 3D distribution extracted each 100 s. In contrast, SWA-HIS contribution is negligible as the ASW acts just as pass through for incoming SWA-HIS telemetry packets. Overall, typically the ASW CPU load is under 40% with a peak of 56% which is reached during RPW-trigger buffer freeze operations.

The data depicted in Fig. 31 are derived from housekeeping data dumped at its maximum frequency of 1 Hz (reporting the ASW processing time) and represents the maximum processing time measured in an observation window of 1 s for the management of each of the four SWA sensors (SWA-EAS1, SWA-EAS2, SWA-PAS, and SWA-HIS), and for the sum of all ASW activities (including the sensor management). In conclusion, the processor does not need to work under stressed conditions. It has more than 40 % margin in the worst case, and the time consumed by the ASW processing tasks is well under its maximum limit of 125 ms. So the risk of breaching operational limits, and the consequent possibility of losing a processing slot and the associated science data is very low (an overrun event report is generated in any such case).

4. SWA science operations

The suite of three SWA sensors plus its SWA-DPU will be operated in a variety of modes in order to address the overall Solar Orbiter mission science goals (Müller et al. 2020; Zouganelis et al. 2020). The SWA operations activities are distributed across three centres, primarily to allow key hardware institutes for the three sensors to address the health and calibration issues of their relevant sensor. The primary SWA operations group is based at UCL MSSL, and will take lead responsibility for SWA-level communications, coordinating activities across the suite, and for processing of the SWA-EAS data products. In this case, "communications" includes liaison and data exchange with the Mission Operations Centre (MOC) at the European Space Operations Centre (ESOC) in Darmstadt, Germany, the Solar Orbiter Science Operations Centre (SOC, Sanchez et al., in prep.) near Madrid, the Solar Orbiter Archive, as well as with partner SWA operations groups in Toulouse (for SWA-PAS related activities) and UMich (for SWA-HIS related activities). This section summarises the key operational issues, mode, and data product information likely to be of use to the scientific user of SWA data.

4.1. SWA telemetry

The baseline operations planning driving the original design of the SWA sensors and their operations was based on returning an orbit average data telemetry rate of ~14.5 kbps. Considering the required data products, the cadences at which they would be required, and the useful duty cycle for higher time resolution (burst mode) data products, a baseline target data production rate for the three sensors was established as ~5.5 kbps for SWA-HIS, ~4.5 kbps for SWA-PAS, ~4.3 kbps for SWA-EAS, and ~300 kbps for the SWA-DPU. Given the uncertainties associated with both the CRs achievable in flight and with the capture of data products associated with irregular triggers, the SWA team planned to maintain broad compliance with these rates by monitoring and internally controlling data taking by the SWA-DPU through the operation of the BKA (see Fig. 30 and associated text). Under this scheme, periods of poor compression ratio or numerous trigger responses would be compensated for by the cancellation of some planned burst mode intervals and switching off of the response to further trigger flags. In extreme cases, autonomous commanding of the sensors into low-cadence data taking would also occur. Conversely, if the sensors supply less data volume to the SSMM (due to a period of efficient data compression or lack of triggers) then the instruments can be commanded to take more burst mode data or to take higher volume data products at higher cadences.

More recent analyses of the mission orbits by the Solar Orbiter project have led to the realisation that there will be times when the instruments can produce significantly more data than the original baseline volumes, and conversely times when data taking cannot proceed at baseline rates without overfilling the SSMM data stores and overwriting previously taken data. For this reason the ESA SOC will, as part of the planning for the mission, define "telemetry corridors" for each instrument. These will define the upper and lower bounds for the data volume acquired by a given instrument at a given point in time. This thus sets the rate, as a function of time, and over periods that may be shorter than the orbital period, at which the instruments may accumulate data. For SWA, the prior existence of the BKA means that this development is readily accommodated in the instrument planning by simply changing the control parameters of the BKA, such that they match the requirements of the telemetry corridors. Although we describe later in this section the various modes and data products produced by SWA, the descriptions are largely based on the nominal behaviour, and we note that a key outcome of the wide range of telemetry rate availability will mean that there will be variances in SWA data cadences and resolutions to accommodate this.

4.2. SWA commanding

SWA commanding is the responsibility of the UCL MSSL SWA operations team, who lead the activity in close consultation with

SWA partners and the SOC. On the basis of mission-level planning by the Solar Orbiter Science Working Team (SWT) and Science Operational Working Group (SOWG), the SWA operations teams will have a baseline operational plan, defining instrument telemetry and power constraints against which to fix the detailed commanding of the three sensors for a given period. In general, the SWA operations team will attempt to plan for the sensors to operate to return the highest volume of best quality science data consistent with those constraints, in particular within the telemetry corridors defined by the SOC. However, coordinated data taking with other instruments (e.g. joint burst mode observations, Walsh et al. 2020) will also be factored in to maximise the potential science return. Compliance of the data taking by the SWA sensors will be monitored and controlled on board by the SWA BKA (see Fig. 30). Instrument operations request (IOR) files will be constructed and submitted to the SOC for compliance testing, before upload to the spacecraft a few weeks before execution.

4.3. SWA modes of operation

4.3.1. SWA-EAS modes of operations

The SWA-EAS instrument can operate in various modes that will return different subsets of the original 3D VDF data. Together with the HK data from each SWA-EAS, there are also various engineering modes that allow instrument health monitoring and fault diagnosis to be performed on a semi-regular basis (about once per week, for a limited duration) in order to ensure that the sensor is maintained in optimum configuration. Of more relevance here are the science modes. These are:

SWA-EAS normal mode. The two SWA-EAS sensors each send their respective sampling of the 3D VDF to the SWA-DPU every second. The SWA-DPU stores these data in a 5 min rolling buffer. Every 4 s the SWA-DPU selects the measurements from each sensor, performs a partial moment calculation (over three subsets of energy range and two angular ranges for each sensor), and adds the resulting 168 parameters to the SSMM for inclusion in the telemetry stream. Optionally, in the event of low counts, the SWA-DPU will add four consecutive measurements from SWA-EAS and then perform the moment calculation. Every 100 s of the full set of $64 \times 32 \times 16$ 3D measurements from each SWA-EAS is compressed and sent to the SSMM. In addition, every 100 s (offset by 50 s from the selection above) a single energy bin slice of the full 3D measurement of each SWA-EAS sensor is compressed and sent to the SSMM for telemetry as a low-latency data product (see Sect. 4.4.5). The data array dimensions for this product are thus $2 \times 1 \times 32 \times 16$;

SWA-EAS burst mode. On command, the SWA-DPU will place the SWA-EAS sensors into burst mode. The SWA-DPU will steer the SWA measurements with reference to the magnetic field unit vector provided by the MAG instrument (Horbury et al. 2020) over the Service 20 IEL feed at 0.125 s cadence. In response, the SWA-EAS sensor whose central plane of FoV passes closest to the magnetic field direction makes measurements at only two elevations (but at full energy and azimuth). These two elevations are chosen such that one set of observations includes the direction along the B-field direction, and the other along the anti-parallel direction. Given that only two elevations are sampled in this mode, the resulting $1 \times 64 \times 32 \times 2$ array of data can be captured every 0.125 s and transmitted to the SWA-DPU for addition to the SSMM and the telemetry stream. These data products will be reassembled on the ground to provide a measurement of the 2D PAD of electrons (with some limited gyrophase information) at 0.125 s cadence.

SWA-EAS triggered mode. Autonomously, and following the receipt of a trigger flag over the Service 20 IEL feed, the SWA-DPU will freeze the rolling buffer containing 5 min of 1 s-cadence samples of the full 3D velocity distribution from each SWA-EAS sensor. The SWA-DPU will transmit the resulting 300 samples of $2 \times 64 \times 32 \times 16$ data arrays to the SSMM for inclusion in the SWA telemetry stream. It is expected that the trigger flag will be set by the RPW instrument (Maksimovic et al. 2020) in response to an autonomous evaluation of whether combined in situ data suggests the passage of an event of scientific interest (e.g. an interplanetary shock) passed the spacecraft in the previous 5 min period.

4.3.2. SWA-PAS modes of operations

SWA-PAS is capable of producing one $96 \times 11 \times 9$ array of data every second. However, due to restrictions of telemetry and power, SWA-PAS will operate in various modes and states that will return different subsets of the original 3D data. These modes are:

SWA-PAS normal mode. SWA-PAS can be operated across a range of parameter space. However, typically in normal mode SWA-PAS will operate on a repeating 300 s cyclogram. The data taking activities during each 300 s cyclogram are illustrated in Fig. 32. The upper part of the figure shows SWA-PAS operation around a 300 s cyclogram boundary, while the lower part shows the operation at each of the two intervening 100 s boundaries. In each case the boundary is marked by the thick vertical dashed lines. The scheme is based on making a measurement of the proton-alpha particle VDF over 1 s every 4 s. This is achieved by taking a series of "normal samples", represented by the grey boxes marked "S" in Fig. 32 over 48 energies, seven azimuths, and five elevations. However, these samples are replaced near the 100 and 300 s boundaries by "full 3D" samples, represented by the orange boxes marked "FS", in which the measurement is extended to all nine elevations. This is to ensure (checked by the SWA-DPU) that the sensor scans to correctly capture the ion distribution in the "normal samples". One such distribution is taken near the 100 s boundary, while two are taken a few seconds before and after each 300 s boundary. Between the latter two full sample measurements, SWA-PAS will be commanded into snapshot mode (see below). Figure 32 also shows, for completeness, the commanding requirements for the scheme (green boxes) and an illustration of the power saving profile (pink lines) in which the sensor voltages are ramped down between measurements. Under this scheme the SWA-PAS sensor makes a sampling of the full 3D VDF of the protons and alpha particles every 4 s, which are passed by the SWA-DPU to the SSMM for telemetry to the ground.

SWA-PAS snapshot mode. For a period of 7 s every 300 s, the SWA-PAS sensor is commanded by the SWA-DPU into snapshot mode. During these periods the sensor will sample over 48 energies, seven azimuths but only three elevations. However, the measurement cadence will be raised to a rate of 4 per second over the 7 s snapshot period. The timing of this mode will be such that it covers the period that the RPW sensor (Maksimovic et al. 2020) will perform its nested snapshot mode. This nested timing of the observations will enable detailed analyses of wave-particle interactions through the combination of high-cadence field and particle measurements.

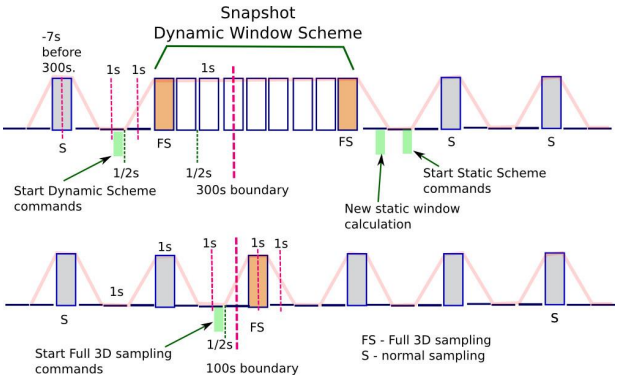

Fig. 32. Schematic illustration of the SWA-PAS cyclogram for data capture during SWA-PAS normal mode (for details see text).

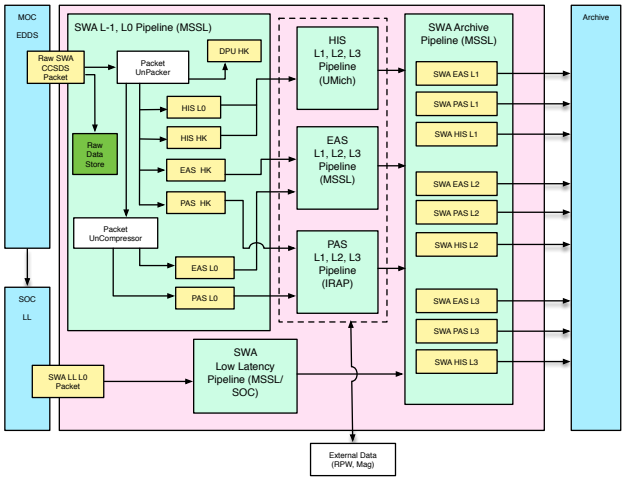

Fig. 33. Schematic of the structure of the SWA data processing pipelines from receipt of telemetry by the MOC to deposit within the ESA science archive.

SWA-PAS burst mode. On command, the SWA-DPU will place the SWA-PAS into burst mode. In this mode SWA-PAS returns samples of the full 3D proton and alpha particle distribution in a variety of formats, and for a limited period depending on telemetry constraints. Typically we expect to be able to support measurements of 48 energies, seven azimuths, and three elevations at 0.25 s cadence for periods of order 5 min. However, more complete samples over all nine elevations can also be made at 1 s cadence over similar periods, depending on scientific goals.

4.3.3. SWA-HIS modes of operations

The SWA-HIS sensor measures heavy ions arriving at the sensor aperture over a range of azimuths and elevations and distributed over a spectrum of energies, together with a measure of the TOF of these particles across a known distance in order to determine species. Each individual heavy ion entering SWA-HIS represents an event. The rates of events over different ranges (energy, elevation, TOF) are recorded, which can form the basis of a determination of a phase space distribution for individual elements. SWA-HIS will provide the full PHA, and the rates of PHA, at different cadences and resolutions since events can be selected to fill the available telemetry rates. The selection algorithm works as follows: All ion event words from an E/q scan are divided into five priority ranges, based on their average abundance in the solar wind. Priority ranges are defined by large Energy-TOF boxes, defined separately for each E/q. Events are chosen at random from each of these ranges, with more events selected from ranges containing less abundant ions. In cases where there are insufficient events present in a given range, that number is added to those to be taken from the next range (and so on). On this basis, we anticipate that in normal mode SWA-HIS will provide packets to the SSMM for telemetry which correspond to a cadence of 30 s for Helium ions and 300 s for heavier ions. Limited periods of burst mode data are possible within the telemetry constraints during which (if there are sufficient counts) Helium data will be returned every 4 s and heavier ions at 30 s. However this mode can only be run on average 1% of the time due to telemetry constraints. Conversely a low-cadence mode will also be employed at larger distances from the Sun or during periods of telemetry restriction, in which the data return would be significantly slower than in normal mode.

SWA-HIS also has a number of engineering modes which, together with the housekeeping data, allows instrument health monitoring and fault diagnosis to ensure that the sensor is maintained in optimum configuration.

4.4. SWA data products

In this subsection we detail the SWA data products that we expect to be made available through the Solar Orbiter Archive for the purposes of supporting the science goals of the mission and the community. It is expected, in accordance with the mission Science Management Plan, that best-effort science-quality level-2 data will be made generally available through the archive at 90 days after the receipt of the relevant telemetry by the ESOC. However, some SWA data products may need additional effort to produce or understanding of calibration parameters may evolve, so it is likely that further releases of the data may occur to update the available data to "current best quality" at various points after the initial release.

The SWA data processing flows from the MOC data delivery service through a series of processing pipelines and back out to the SOC archive and other archives as illustrated in Fig. 33. There are six distinct pipeline elements (shaded light green in the figure) dealing with the processing and calibration of the various data products collected by the three SWA sensors and distributed among the SWA operations teams at UCL MSSL, IRAP, and UMich. The remainder of this section provides a top level description of the data types and products produced from these pipelines.

4.4.1. SWA house-keeping and engineering data

The sensor teams for all three of the science sensors within SWA, and the SWA-DPU team have defined a set of house-keeping and engineering parameters for priority download from the spacecraft. It is anticipated that these are available immediately after the ground station pass following their acquisition. An archive of these data products will be maintained by the instrument teams and the project, although it is not foreseen that these will routinely be released to the wider community. However, these data can be made available to researchers should a specific need be identified.

4.4.2. SWA Level 0 and Level 1 data

Data collected by the SWA sensors and SWA-DPU are returned in the telemetry stream as individual CCSDS packets. Once on the ground, these packets are decommutated into relevant files

containing the separate SWA-EAS, SWA-PAS, and SWA-HIS data, and uncompressed to form the L0 raw data packets. These files are still in CCSDS format and are saved and archived in binary format. The process used to create these data files is a simple C code that searches on the data type, subtype, and SID. Data which are compressed are passed through a decompressor. The decommutated and uncompressed CCSDS packet files are grouped into appropriate files for each sensor and each 24 h period. They are stored at UCL MSSL and made available to the wider SWA team.

The SWA L1 data are the uncalibrated, uncompressed L0 data converted into CDF format. The individual sensor teams are responsible for generating SWA L1 data from the L0 packets. These CDF files will have the CCSDS header data and the CCSDS science data combined. All data products are stored as CDF files according to "SOL-SGS-TN-0009 Metadata Definition for Solar Orbiter Science Data". As well as being stored in the SWA Master Repository at UCL MSSL with the L0 data, these files will be be converted to NetCDF format to fit the AMDA tool specification and stored in the Centre de Données de la Physique des Plasmas (CDPP) data archive.

SWA-EAS L1 data. UCL MSSL is responsible for generating the SWA-EAS L1 data from the L0 source. The SWA-EAS L1 data products are, for each SWA-EAS sensor, as follows:

– Normal Mode Spectra in counts, one set for each SWA-EAS sensor. The angular bin directions are in the SWA-EAS sensor reference frames;

– Burst Mode spectra in counts, from one sensor viewing the magnetic field direction. The angular bin directions are in the relevant SWA-EAS sensor frame;

– Triggered Mode Spectra in counts, one set for each SWA-EAS sensor. The angular bin directions are in the SWA-EAS sensor reference frames. These data are at the highest cadence of one 3D sweep per second for a period of 5 min;

– Partial moments calculated on board (6 sets per SWA-EAS sensor) in physical units. The frame references are the SWA-EAS sensor reference frames;

– Engineering mode and calibration data.

SWA-PAS L1 data. IRAP is responsible for generating the SWA-PAS L1 data from the L0 source. The SWA-PAS L1 data products are as follows:

– Normal Mode Spectra in counts. The angular bin directions are in the SWA-PAS frame;

– Normal Mode Snapshot Spectra. The angular bin directions are in the SWA-PAS frame;

– Burst Mode spectra. The angular bin directions are in the SWA-PAS frame;

– Onboard moments in physical units and in the SWA-PAS frame of reference;

– Engineering and Calibration data;

An example of the expected output from the SWA-PAS sensor is shown in Fig. 34. We used the SWA-PAS Proto-Flight Model (PFM) calibration data to simulate the SWA-PAS response, together with very high sampling rate solar wind data from the Faraday cup instrument BMSW onboard of RadioAstron mission (Šafránková et al. 2013) as an input for the simulation. The resulting E-T colour-coded spectrogram in the lower panel of the figure illustrates to the expected output in the SWA-PAS normal mode when the instrument takes a full 3D ion VDF every 4 s.

To illustrate the SWA-PAS ability to resolve the proton and He^{2+} peaks, we have made also a realistic simulation of SWA-PAS energy spectra for two different solar wind conditions

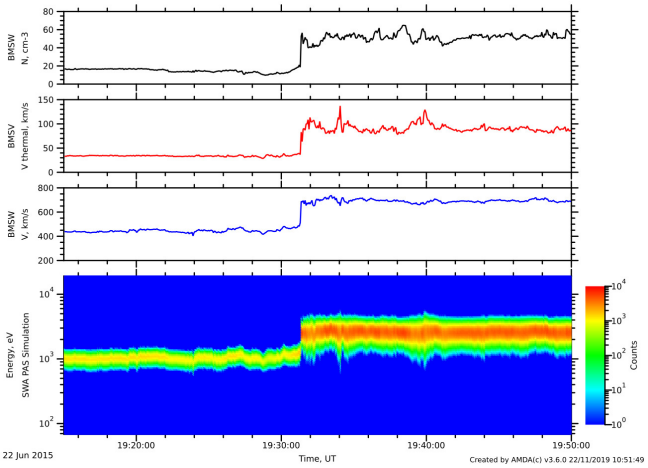

Fig. 34. Simulation of a SWA-PAS Energy-Time Spectrogram. *Three top panels*: input parameters to the simulation as measured by the BMSW instrument onboard the RadioAstron mission. *Bottom panel*: expected sensor response integrated over all angular bins. The time of the measurements is shifted relative to UT by about 1.5 h.

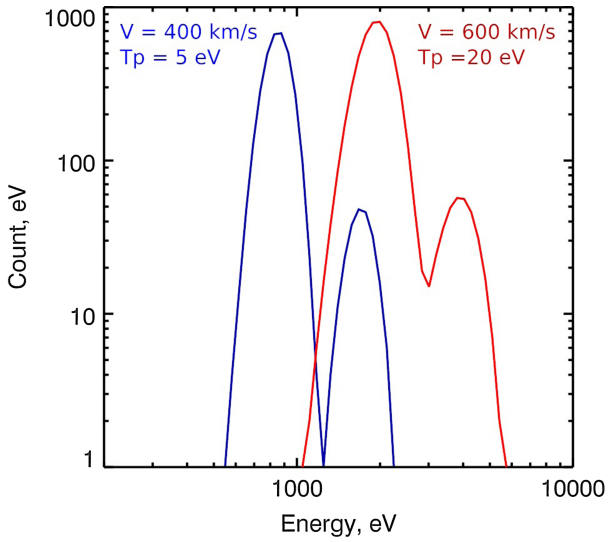

Fig. 35. Simulated examples of SWA-PAS energy spectra for different solar wind conditions. The temperature of He^{2+} peak is assumed as Tp × 4.

(Fig. 35). In both cases the He^{2+} temperature is factor 4 higher than proton temperature. We can see that the He^{2+} peak should be easily resolved by the sensor.

SWA-HIS L1 data. UMich is responsible for generating the L1 SWA-HIS data from the L0 source. These data will be in CDF format. SWA-HIS L1 data products are as follows:

– Ion Event (PHA) words: Individual ion event data, containing full information on incident angles (elevation and azimuth), E/q, TOF, and SSD energy in digital units. The number of PHA words telemetered for each energy scan is fixed (the same for each scan) but configurable, based on available resources. A sampling algorithm is employed to select the sample sent to the ground (see Sect. 4.3.3).

– Priority Rates: Counts of PHA events within a priority range, as a function of E/q and elevation. See below for description of typical use;

– Sensor Rates: Counts of unclassified ion event words on the SWA-HIS detectors (start MCP, stop MCP, SSD) as a

function of E/q, integrated over incident angles, TOF, and Energy. Includes full counts of events subject to decimation. Sensor rates also include two coincidence rates, the number of events with a valid TOF and energy (triple coincidence), and a count of those with only a valid TOF (double coincidence). These rates are primarily used to evaluate the performance of the instrument, rather than for science. In particular, they can be used for calculation of ion detection efficiency in-flight (von Steiger et al. 2000);

– Decimation Rates: Counts of ion event words in each of three decimation ranges as a function of E/q. In order to reduce the on-board processing load caused by light ions and low-TOF noise sources, only a fraction (1 in N) of those events are transmitted to the SWA-HIS C&DH board from the HV bubble. Separate decimation ranges in E/q and TOF are included for alpha particles, protons, and low-TOF events caused by accidental coincidences. The fraction transmitted is commandable, from typically one in four for alphas to zero for low-TOF noise events;

– Matrix Rates: Counts of ion event words within a specified Energy-TOF range, classified and counted onboard, for each E/q step. These are summed over incident angle. SWA-HIS has 32 such species boxes intended to roughly select counts of ion event words measured for particular ion species. Classification transforms E/q, TOF, and residual energy into the two dimensions of Energy and TOF. Classification is primarily used for other data products (below and in low-latency). This data product is not in telemetry for most instrument data rates. If resources allow, He^{2+}, C^{4-6+}, O^{6-7+}, and Fe^{10+} ions may be included. Additional ions and charge states may be produced according to science needs and as counting statistics allow;

– Rate-Based VDFs: Counts of ion event words for a set of ions subdivided by E/q, elevation, and azimuth. The selection of ions will include He^{2+}, C^{5+}, O^{6+}, and Fe^{10+}. Additional ions and charge states may be produced according to science needs and as counting statistics allow. Since these counts are not subject to the effect of the priority sampling algorithm, they represent the best possible statistics. However, because species are separated simply by boxes and no peak overlap removal is performed (see below), the counts are not as accurately assigned to a given species as they would be if formed on the ground, especially for lower abundance heavy ions;

– Engineering and calibration data.

4.4.3. SWA Level 2 data

We define SWA L2 data products as those that have been fully processed and calibrated such that parameters have physical units and are in a common, scientific frame of reference. These are intended as the primary science quality data sets from the SWA project, and the intention is to release these products to the open Solar Orbiter Mission Archive at 90 days after the receipt of the corresponding telemetry from the spacecraft, consistent with the requirements of the mission Science Management Plan. The validation of some L2 data products requires information from other instruments on the spacecraft (e.g. the spacecraft potential measure from RPW and the B-field unit vector from MAG) or extended periods of data taking to validate calibration parameters (e.g. for very low flux heavy ion populations) which may compromise science quality at 90 days and necessitate later updates to the data products.

All SWA L2 data products will be placed, with appropriate metadata, within CDF files according to the format specified in "SOL-SGS-TN-0009 Metadata Definition for Solar Orbiter Science Data". The L2 files from all three SWA sensors will be collected and stored in the SWA master repository at UCL MSSL, along with the auxiliary data generated from the mission. These data files will be submitted to the official ESA Solar Orbiter Archive, from where they will be shared with the NASA Space Science Data Coordinated (NSSDC) archive and the CDPP data archive in France. These files may also be converted by the UCL MSSL team to appropriate format (e.g. NetCDF format to fit the AMDA tool specification) as requested by the archives.

In the remainder of this subsection we provide an overview of the SWA L2 data products that we expect to be readily available from the archive and suitable for science purposes. Full details can be found in SWA technical documentation, particularly the SWA Data Product Definition Document (SO-SWA-MSSL-IF-006).

SWA-EAS L2 data. The Operations team at UCL MSSL is responsible for generating SWA-EAS L2 data. The generation of the full set of SWA-EAS L2 data products from the L0 data products depends a number of sources of auxiliary information including:

– SWA-EAS ground calibration files held at UCL MSSL;

– SWA-EAS flight calibration files, regularly updated during the mission from ESA L0 engineering and calibration data and held at UCL MSSL;

– Spacecraft orbit and attitude information files (e.g. SPICE kernels) available from the SOC;

– Spacecraft potential data associated with each set of SWA-EAS moment calculations (i.e. at 4 s cadence), provided by the RPW instrument;

– Magnetic field direction associated with each SWA-EAS burst mode sample (i.e. at 0.125 s cadence), provided by the MAG instrument.

The set of SWA-EAS L2 data products includes the following primary scientific outputs:

– Onboard moments: A complete set of 14 parameters comprising the best estimation of the moments of the electron velocity distribution (i.e. density, bulk velocity vector, components of the pressure tensor, heat flux vector, and including total counts in the distribution) available from the onboard-generated L1 moments data. This product is available for periods in which the SWA-EAS sensors are in normal mode, and will be provided in physical units and in a relevant heliospheric reference frame. This product will be produced by appropriately combining the L1 partial moments data from each sensor including reference to the spacecraft potential from RPW in order to minimise the effect of spacecraft charging and presence of photo- and secondary electrons of spacecraft origin. The data product will be available at 4 s time resolution;

– Full 3D electron distributions: Electron distributions expressed as a VDF, differential energy flux, and differential number flux provided with appropriate physical units and in a relevant heliospheric reference frame. These distributions are produced by appropriately combining spectra from the two sensors, taking into consideration those parts of the FoV which have an overlap between the two SWA-EAS sensors. In their fullest form these data products will cover the energy range 1 eV−5 keV in 64 energy steps, and with the two orthogonally-mounted sensors each covering ±45° and ±180° in elevation (in 16 steps) and azimuth (in 32 steps), the combined system is capable of covering more than the full 4 π steradian FoV. Measurements at low energy steps contaminated by photo- and secondary electrons will be replaced by fill values, as well as angular bins which may have been affected by a blockage to arrival electrons

by the spacecraft and its appendages. These products are available for periods in which the SWA-EAS sensors are in normal mode. The nominal time resolution for these data products is 100 s, although they can be made available with 10 s resolution when the spacecraft is relatively close to the Earth and higher than average telemetry rates can be made available. Conversely, these products may only be available at 400 s resolution during periods when the project needs to limit overall telemetry below the baseline allocation to instruments;

– Ground moments: A complete set of 14 parameters comprising the ground-calculated moments of the electron VDF (i.e. density, bulk velocity vector, components of the pressure tensor, heat flux vector, and including total counts used to derive the distribution). This product is generated from the normal mode combined 3D electron distributions following calibration and correction for the spacecraft potential derived from RPW data. These data products will have two variants, the moments resulting from both a direct moment summation across the corrected and validated full 3D VDF and, where appropriate, a fit to a model core, halo, and strahl distribution. This product is again available for periods in which the SWA-EAS sensors are in normal mode, and will be provided in physical units and in a relevant heliospheric reference frame. It will be generated on the same resolution as the available 3D VDF's (i.e. nominally at 100 s time resolution, but with variants at 10 s and 400 s depending on telemetry rates);

– Trigger Mode distributions: Full 3D electron distributions derived from L0 data captured and telemetered to ground in response to a freeze of the internal SWA rolling memory buffer following the receipt and acceptance by the SWA-DPU of an appropriate trigger flag via the S20 inter-instrument communications link from RPW. This "trigger mode" data product will be assembled in the same way as the normal mode full 3D distributions functions discussed above (i.e. combined data from both sensors) but will be available at 1 s cadence for a period of 5 min per triggered event. As for the normal mode distributions, these data will be available in appropriate physical units expressed as a VDF, a differential energy flux, and a differential number flux, each in a relevant reference heliospheric frame.

– Trigger Mode Moments: These moment parameters are calculated on the ground in the same way as the "Ground Moments" described above, but are derived from the combined trigger mode VDF's following calibration and correction for the spacecraft potential derived from RPW data. They will thus be available at 1 s time resolution over the trigger mode periods of 5 min per event accepted by the SWA-DPU;

– Burst mode electron pitch angle (2D) distributions: SWA-EAS data collected in burst mode, comprising two full azimuth scans from two elevations from one sensor, will be rebinned into pitch angle space on the ground with reference to the validated magnetic field unit vector. The resulting 2D electron pitch-angle distributions thus will be delivered in physical units (in distribution function, differential energy flux, and differential number flux formats), and in a frame defined by the magnetic field direction. The data product can contain up to 64 energy bins and 64 pitch angle bins, although these will likely be reduced in size by removing energy bins contaminated by photo-electron fluxes and combining the individual pitch angle measurements into a regular set of pitch angle bins. The time cadence of this product is 0.125 s, and it will generally be available for limited periods (average of less than 12 min per day) due to telemetry constraints. Longer periods may be available during enhanced telemetry periods or by reducing the duty cycle and combining available burst mode periods over a longer period of time;

– Single energy angle-angle electron distributions: This data product is equivalent to the ground validated and enhanced SWA-EAS low-latency data product (see Sect. 4.4.5). It is available for periods in which the sensor operates in normal mode, and contains a full angular distribution (i.e. combined data from both sensors) for a single energy bin, usually chosen in the range expected for the solar wind strahl population. The data product will be made available in physical units (in distribution function, differential energy flux, and differential number flux formats), and in a relevant heliospheric frame. The raw L0 data forming the corresponding low-latency product is only available at a time resolution 100 s. However, given the operation of the sensor to capture that product between measurements of the normal mode VDF's the ground produced L2 version of this product will usually be available at 50 s time resolution or better;

SWA-PAS L2 data. The SWA operations team at IRAP, Toulouse, is responsible for generating SWA-PAS L2 data. The generation of the full set of SWA-PAS L2 data products from the L0 data products depends a number of sources of auxiliary information including:

– L0 data products;
– SWA-PAS ground calibration files;
– SWA-PAS flight calibration files (Obtained from L0 data);
– Spacecraft orbit and attitude information files (e.g. SPICE kernels);

The set of SWA-PAS L2 data products includes the following primary scientific outputs from the SWA-PAS sensor:

– Full and reduced 3D ion distributions: Ion distributions expressed in scientific units (as differential fluxes and as VDFs), and in a relevant physical frame (e.g. the solar-ecliptic frame). These data are available from periods of normal mode operation, usually with 4 s time resolution;

–Snapshot mode fast 3D ion distributions: Ion distributions obtained during periods of snapshot operation expressed in scientific units (as differential fluxes and as VDFs), and in a relevant physical frame. Snapshot mode measurements are made at a cadence of one distribution per second over a period of 7 s, recurring every 300 s during normal mode operation;

– Burst Mode fast 3D ion distributions: Ion distributions obtained during periods of burst mode operation expressed in scientific units (as differential fluxes and as VDFs), and in a relevant physical frame. SWA-PAS burst mode measurements can be made at a variety of cadences (extending down into the sub-second range) depending on the trade-off between time and angular or energy resolution. The duration of the burst mode period is variable, depending on available telemetry, but will generally occur in 5 min periods. Details of the operation for a given burst mode interval will be included in the meta-data for the data product.

– Ground-calculated H^+ moments: The 3D ion distributions will be appropriately processed on the ground to produce moments (density, bulk velocity, pressure tensor) for the proton component of the solar wind captured by SWA-PAS. Data will be in scientific units in an appropriate physical reference frame, and will generally be available with 4 s cadence;

– Ground-calculated He^{2+} moments: As above for protons, but separating out the moments for the alpha particle component of the solar wind capture by SWA-PAS;

– Onboard-calculated Moments: This data product is essentially the ground-validated SWA-PAS low-latency data product (see Sect. 4.4.5). It is provided for reference, but essentially

Table 9. SWA-HIS Level 2 derived data products in physical units.

Data product	Time resolutions [1]
Ion event (PHA) words	30 s, 300 s, 4 s [2]
E/q (keV/e)	
Elevation and azimuth (deg)	
Time-of-flight (ns)	
Total energy (keV)	
Priority range	
Decimation range	
Sensor rates (flux)	30 s, 300 s, 4 s [2]
Start	
Stop	
SSD	
Double coincidence	
Triple coincidence	
Normalisation rates	30 s, 300 s, 4 s [2]
Decimation	
Priority	
Matrix rates [3]	30 s, 300 s, 4 s [2]
He^{2+}	
C^{4-6+}	
O^{6-7+}	
Fe^{10+}	
Rate-based velocity distributions [3]	
He^{2+}	30 s, 300 s, 4 s [2]
C^{5+}	30 s, 300 s, 4 s [2]
O^{6+}	30 s, 300 s, 4 s [2]
Fe^{10+}	30 s, 300 s, 4 s [2]

Notes. [1]These are the possible time resolutions. For some periods in the solar wind, the highest time-resolution will not provide data with sufficient statistical accuracy. The best, most scientifically useful averaging intervals will be determined ground analyses of the counting accuracy achievable. [2]Data at this resolution corresponds to SWA-HIS Burst mode, which can only be run on average 1% of the time due to telemetry constraints. [3]Data product not included for most telemetry rates.

is superceded in terms of quality by the ground-calculated moments described above.

SWA-HIS L2 data. The SWA operations team at UMich is responsible for generating SWA-HIS L2 data. The generation of the full set of SWA-HIS L2 data products from the L0 data products depends a number of sources of auxiliary information including:

– L0 data products;
– SWA-HIS ground calibration files;
– SWA-HIS flight calibration files (Obtained from L0 data);
– Spacecraft orbit and attitude information files (e.g. SPICE kernels);

The set of SWA-HIS L2 data products is summarised in Table 9 and includes the following primary scientific outputs from the SWA-HIS sensor:

– Ion event (PHA) words: Full information about measured ion events, including E/q, TOF, energy, and incident angles (elevation and azimuth) in physical units. These are the primary science data product from SWA-HIS, and make up the bulk of SWA-HIS telemetry volume in normal and low cadence modes;

– Priority rates: Total counts of ion event words in each priority range, divided by E/q and elevation angle bin. (Duplicate of L1 version). These rates are used to correct the weighting of telemetered ion event words for the effect of the sampling algorithm. For example, if the priority rate for a given E/q step and elevation bin is ten, but only five of these ion event words were included in telemetry, then each counts for two in further processing;

– Sensor rates: L1 sensor rates converted to differential number flux units, $(cm^2\ s\ sr\ keV)^{-1}$;

– Decimation rates: Duplicate of L1 version since conversion to flux units is not useful;

– Matrix rates: L1 Matrix Rates converted to number flux units, $(cm^2\ s)^{-1}$;

– Rate-based VDFs: L1 Rate-Base VDFs converted to differential number flux units, $(cm^2\ s\ sr\ keV)^{-1}$.

4.4.4. SWA Level 3 data

It is anticipated that during the course of the mission the primary science data products, as represented by the SWA L2 data products submitted to the archives and discussed above, will be supplemented by the creation of higher order, or Level 3, SWA data products. These products may arise either through further reduction of the L2 products or perhaps through further combinations of data products either within the SWA suite or with other instruments on Solar Orbiter. For SWA-EAS and SWA-PAS, possible examples of this might include SWA-EAS PADs generated from the Trigger Event 3D distributions with reference to the magnetic field direction (providing a cadence of 1 s for a 5 min period), or electron or ion moments calculated over narrower energy ranges, etc.

In the case of SWA-HIS, the most accurate and scientifically useful data products are formed via a peak overlap removal algorithm to assign counts to individual ion species in ground processing (von Steiger et al. 2000; Shearer et al. 2014). This algorithm uses a forward model to predict the peak centre location of each of the >75 analysed ions in TOF – energy space at each E/q step. This forward model, which includes estimated peak width as well as centre, is developed from ground calibration and in-flight accumulated data. A set of two-dimensional Gaussian curves is formed from these centres and widths and provides an initial estimate of count vectors assigned each species. A maximum-likelihood estimation (MLE) method then shuffles counts among these vectors to remove overlap in the statistically optimal way. Events at each pair of incident angle bins are processed independently to preserve distributions in these dimensions. Count vectors from all angle bins are then recombined and converted to phase-space density ($s^3\ km^{-6}$) to form 3D VDFs. Moments of density, velocity, and temperature are then computed from these VDFs and used to produce the following data products from SWA-HIS (see Table 10):

– Elemental abundances: This data product contains the sum of all ion densities for a particular element provided as a ratio to those of oxygen;

– Ionic charge states: Density ratios for specified ion pairs or average charge states, computed as density-weighted average;

– Charge state distributions: Normalised distribution of all charge states analysed for a specified element;

– Kinetic properties: Moments of VDFs for specified ions. This data product includes the density (cm^{-3}), bulk velocity ($km\ s^{-1}$), and temperature (K) for the specified ions;

– Velocity distributions: Phase space density ($s^3\ km^{-6}$) of the specified ions in instrument frame, binned according to speed and incident angles (elevation and azimuth).

Table 10. SWA-HIS Level 3 derived data products in physical units.

Data product	Time resolutions [1]
Elemental abundances	
Fe/O	30 s, 300 s, 4 s [2]
C/O	30 s, 300 s, 4 s [2]
He/O	30 s, 300 s, 4 s [2]
Mg/O	30 s, 300 s
Si/O	30 s, 300 s
Ne/O	30 s, 300 s
S/O	>300 s [2]
N/O	>300 s
Ionic charge states	
O^{7+}/O^{6+}	30 s, 300 s, 4 s [2]
C^{6+}/C^{4+}	30 s, 300 s, 4 s [2]
C^{5+}/C^{4+}	30 s, 300 s, 4 s [2]
$\langle Q_O \rangle$	30 s, 300 s, 4 s [2]
$\langle Q_C \rangle$	30 s, 300 s, 4 s [2]
$\langle Q_{Fe} \rangle$	30 s, 300 s, 4 s [2]
Ionic charge state distributions	
$Q_i(O)$, $i = 5, \ldots, 8$	30 s, 300 s
$Q_i(C)$, $i = 4, \ldots, 6$	30 s, 300 s
$Q_i(Fe)$, $i = 6, \ldots, 20$	30 s, 300 s
$Q_i(Si)$, $i = 6, \ldots, 12$	30 s, 300 s
$Q_i(Ne)$, $i = 8, \ldots, 10$	30 s, 300 s
$Q_i(Mg)$, $i = 5, \ldots, 12$	30 s, 300 s
$Q_i(N)$, $i = 5, 6$	30 s, 300 s [3]
$Q_i(S)$, $i = 6, \ldots, 14$	30 s, 300 s [3]
Bulk properties (n, v_{bulk}, T)	
He^{2+}	30 s, 300 s, 4 s [2]
C^{5+}	30 s, 300 s, 4 s [2]
O^{6+}	30 s, 300 s, 4 s [2]
Fe^{10+}	30 s, 300 s, 4 s [2]
Velocity distributions [4]	
He^{2+}	30 s, 300 s, 4 s [2]
C^{5+}	30 s, 300 s, 4 s [2]
O^{6+}	30 s, 300 s, 4 s [2]
Fe^{10+}	30 s, 300 s, 4 s [2]

Notes. [1]These are the possible time resolutions. For some periods in the solar wind, the highest time-resolution will not provide data with sufficient statistical accuracy. The best, most scientifically useful averaging intervals will be determined by ground analyses of the counting accuracy achievable. [2]Data at this resolution corresponds to SWA-HIS Burst mode, which can only be run on average 1% of the time due to telemetry constraints. [3]These elements are more difficult to resolve. Appropriate time resolutions will be determined in flight. [4]Additional charge states may be produced during periods of high counting statistics.

It is expected that some elements of the processing or analyses of the SWA sensor data will in time become routine. In such cases, the SWA operations teams will include these in the SWA processing pipelines and the results will be stored in the master SWA archive at UCL MSSL and submitted to the archives with the corresponding level 2 data.

4.4.5. SWA low-latency data

The Solar Orbiter project reserved a small amount of telemetry within the download budget for priority download of a subset of the data from each of the instruments on board the spacecraft. These data are downloaded from the instrument packet stores with priority second only to the house-keeping data. It is thus anticipated that these data would also normally be available immediately after the ground station pass following their acquisition, and thus with a latency which will generally be low in comparison to that of the full, regular instrument data set for the same observing period. For this reason, the volume of such low-latency data generated by each instrument is very limited ($\sim$1 Mbyte day^{-1}), corresponding to a maximum of $\sim$100 bits s^{-1} within each instruments telemetry stream.

The primary purpose of the low-latency data is to aid in the "last-minute" pointing of the remote sensing instruments on the platform, although there are also obvious benefits to instrument operation to have visibility of the science data production with short turn-around times. However, this also has potential uses as a "space weather beacon" data set, and indeed to provide some context for early identification and assessment of periods of potentially high scientific interest (e.g. for those instruments that may wish to use a selective data download capability). Given these "fast-turnaround" functions, the low-latency data from SWA will be produced immediately after receipt of the telemetry by an automated pipeline within a virtual machine which has been delivered to the ESA SOC. It will be made available immediately to the community through the Solar Orbiter archive.

The specific SWA low-latency data products that, at the time of writing, are intended to be made available are described below:

SWA-EAS. Following acquisition of a full 3D VDF from the two SWA-EAS sensor heads, the SWA-DPU will, with 100 s cadence, select a single (ground-commandable) energy level and extract all electron counts from all angular bins for both heads. The resulting data (2 heads $\times$ 32 azimuths $\times$ 16 elevations $\times$ 1 energy $\times$ 2 byte words compressed by factor 4 every 100 s $\sim$ 43 bits s^{-1}) will be added to the SWA low-latency telemetry stream. In flight it is intended that the SWA-DPU will select an energy in the range which generally isolates the strahl population in the solar wind, and thus has been termed "single (strahl) energy distribution". Thus after processing by the SOC virtual machine, this low-latency data product should indicate the presence (or not) of narrow beams directed parallel or anti-parallel to the magnetic field direction, which provides key information indicating the nature of the connection of the magnetic field line passing through the spacecraft location to the Sun. We note also that this data product will be derived from a full 3D distribution measurement that otherwise would not fall in the downloaded normal mode data (see below). Thus this SWA-EAS single (strahl) energy distribution product will be offset by 50 s from the 100 s cadence full 3D data product. This is in order to avoid duplication of telemetered data and to allow subsequent on-ground data processing to generate an equivalent data product at twice the cadence ($\sim$50 s). The data product can only be generated while the SWA-EAS sensor is in normal mode.

SWA-PAS. From the SWA-PAS normal mode measurements, the SWA-DPU will calculate on board a set of proton and alpha particle moments every four seconds. These SWA-PAS moments will consist of a single density value, a 3-element velocity vector, and a 9-element pressure tensor, which will be added to the SWA low-latency telemetry stream, where they typically require $\sim$46 bits s^{-1}. This data product will regularly provide the community with near-immediate (<1 day delay) context of the solar wind conditions (fast or slow stream, etc.) at the spacecraft.

SWA-HIS. SWA-HIS will contribute four items to the low-latency telemetry stream, one charge state ratio, one elemental abundance ratio, and two rate spectra. The charge state and elemental abundance ratios will be on-board computed versions of those described in the L3 data products (above). The rate spectra will be selected from one of the sensor or matrix rates. These data, normally containing a total of 131 8-bit words, will be sent every 300 s, contributing 4 kbps to the telemetry stream, including packet overhead (although an option for 30 s cadence is available). These can be used for payload-wide science planning and end-to-end instrument health monitoring. Charge state and elemental abundance ratios enable monitoring of solar wind type (slow, fast, shock) and baseline tracking of structures in the solar wind, while the rate spectra are a valuable measure of the plasma environment and the correct end-to-end operation of the SWA-HIS sensor.

5. Summary and conclusions

The SWA instrument is a suite of scientific sensors on-board Solar Orbiter that is designed and developed to measure the thermal and suprathermal charged particle populations in the inner heliosphere. SWA is comprised of three distinct sensor systems, plus a coordinating SWA-DPU, or electronics box, which together will make key measurements of electron, protons and alpha particle, and heavy ion populations arriving at the spacecraft location. Details of the sensor designs and characteristics have been summarised in this paper: SWA-EAS is located in the spacecraft shadow at the end of the boom, and is capable of detecting electrons arriving from all directions (except those blocked by the spacecraft or its appendages) across the energy range of 1 eV to ~5 keV. The SWA-PAS samples protons and alpha particles with energies in the range 0.2–20 keV/e arriving from within a few tens of degrees of the solar direction. Given the ratio of the solar wind bulk flow speed to the proton thermal speed, this FoV through a cut-out in the spacecraft heat shield is sufficient to capture the full distribution of arriving particles under most expected circumstances. The SWA-HIS samples and categorises heavy ions (masses from He to Fe) with energies in the range <0.5–100 keV/e, also arriving from within a few tens of degrees of the solar direction. The sensor is also located behind the spacecraft heat shield with a FoV extending through a cut out in one corner. Finally, the SWA-DPU provides all sensor commanding and control functions, power supply, and data processing for SWA-EAS and SWA-PAS and data communications from all sensors to the spacecraft SSMM, as well as monitoring sensor operations and health.

The broad range of operating modes and data products expected from the suite of sensors have also been described in this paper. Normal mode data products, including electron on-board-calculated moments and proton and alpha particle velocity distributions, are expected to be available on a time cadence of 4 s. Electron velocity distributions and heavy ion composition and charge state information will generally be available at a lower cadence (normally ~100 s and ~300 s respectively, due to telemetry restrictions or expected count rates), but each of these data products is expected to make a key contribution to the scientific objectives of the mission. In particular, SWA has a critical role in establishing the links between measurements made by the in situ instruments on the spacecraft and those remote sensing instruments observing potential source regions of the solar wind, either through establishing solar wind speed by which to map solar wind streamlines back to the Sun, through comparison of ion composition and FIP information to verify connections, to the presence of electron strahl to establish magnetic connections to the Sun. Moreover, the SWA sensors will operate in several possible burst modes and triggered modes (at sub-second cadences for SWA-EAS and SWA-PAS and down to 4 s for SWA-HIS) which will provide unique inputs to mission goals that focus on solar wind kinetics, turbulence, and the nature of relatively small-scale structures.

In all cases, the SWA sensors, as delivered to the spacecraft, meet or exceed the performance requirements originally set out to achieve the mission science goals. The successful operation of the SWA sensors throughout the course of the Solar Orbiter mission will result in the provision to the solar and heliospheric science community of unique data products revealing the nature of the solar wind depending on both heliocentric distance and solar latitude. The SWA data will underpin efforts to link the in situ measurements of the solar wind made at the spacecraft with remote observations of the candidate source regions. This will lead to very significant advances in our understanding of the mechanisms accelerating and heating the solar wind, driving eruptions and other transient phenomena on the Sun, and controlling the injection, acceleration and transport of the energetic particles in the heliosphere.

Acknowledgements. The Solar Orbiter Solar Wind Analyser (SWA) scientific sensors, SWA-EAS, SWA-PAS, SWA-HIS, and the SWA-DPU have been designed and created, and are operated under funding provided in numerous contracts from the UK Space Agency (UKSA), the UK Science and Technology Facilities Council (STFC), the Agenzia Spaziale Italiana (ASI), the Centre National d'Etudes Spatiales (CNES, France), the Centre National de la Recherche Scientifique (CNRS, France), the Czech contribution to the ESA PRODEX programme, and NASA. The very significant efforts by a wide team of engineers, scientists, industrial partners, and subcontractors to the development of the instrument suite are gratefully acknowledged.

References

Auchère, F., Andretta, V., Antonucci, E., et al. 2020, A&A, 642, A6 (Solar Orbiter SI)
Bale, S. D., Kasper, J. C., Howes, G. G., et al. 2009, Phys. Rev. Lett., 103, 211101
Carlson, C. W., & McFadden, J. P. 2013, Design and Application of Imaging Plasma Instruments (American Geophysical Union (AGU)), 125
Carlson, C., Curtis, D., Paschmann, G., & Michel, W. 1982, Adv. Space Res., 2, 67
Collinson, G. A., & Kataria, D. O. 2010, Meas. Sci. Technol., 21, 105903
Dusenbery, P. B., & Hollweg, J. V. 1981, J. Geophys. Res., 86, 153
Feldman, U., & Widing, K. 2003, Space Sci. Rev., 107, 665
Feldman, W. C., Asbridge, J. R., Bame, S. J., Montgomery, M. D., & Gary, S. P. 1975, J. Geophys. Res., 80, 4181
García-Marirrodriga, C., Pacros, A., Strandmoe, S., et al. 2020, A&A, in press, https://doi.org/10.1051/0004-6361/202038519 (Solar Orbiter SI)
Gary, S. P. 1991, Space Sci. Rev., 56, 373
Gary, S. P. 1993, Theory of Space Plasma Microinstabilities (Cambridge, UK: Cambridge University Press), 193
Gary, S. P., & Karimabadi, H. 2006, J. Geophys. Res.: Space Phys., 111, A11224
Gary, S. P., Feldman, W. C., Forslund, D. W., & Montgomery, M. D. 1975, J. Geophys. Res., 80, 4197
Gary, S. P., Montgomery, M. D., Feldman, W. C., & Forslund, D. W. 1976, J. Geophys. Res., 81, 1241
Gary, S. P., Foosland, D. W., Smith, C. W., Lee, M. A., & Goldstein, M. L. 1984, Phys. Fluids, 27, 1852
Gary, S. P., Yin, L., Winske, D., & Reisenfeld, D. B. 2000, Geophys. Res. Lett., 27, 1355
Gloeckler, G., Zurbuchen, T., & Geiss, J. 2003, J. Geophys. Res.: Space Phys., 108, A4
Hellinger, P., Trávníček, P., Kasper, J. C., & Lazarus, A. J. 2006, Geophys. Res. Lett., 33, L09101
Horbury, T. S., O'Brien, H., Carrasco Blazquez, I., et al. 2020, A&A, 642, A9 (Solar Orbiter SI)
Hundhausen, A. J., Gilbert, H. E., & Bame, S. J. 1968, J. Geophys. Res. (1896–1977), 73, 5485
Isenberg, P. A., & Hollweg, J. V. 1983, J. Geophys. Res., 88, 3923
Johnstone, A., Alsop, C., Burge, S., et al. 1997, Space Sci. Rev., 79, 351

Kessel, R., Johnstone, A., Coates, A., & Gowen, R. 1989, Rev. Sci. Instrum., 60, 3750
Klein, K. G., & Chandran, B. D. G. 2016, ApJ, 820, 47
Ko, Y., Fisk, L., Geiss, J., Gloeckler, G., & Guhathakurta, M. 1997, Sol. Phys., 171, 345
Laming, J. M. 2015, Liv. Rev. Sol. Phys., 12, A2
Landi, E., Gruesbeck, J. R., Lepri, S. T., & Zurbuchen, T. H. 2012, ApJ, 750, A159
Lynch, B. J., Reinard, A. A., Mulligan, T., et al. 2011, ApJ, 740, A112
Maksimovic, M., Bale, S. D., Chust, T., et al. 2020, A&A, 642, A12 (Solar Orbiter SI)
Marsch, E. 2006, Liv. Rev. Sol. Phys., 3, 1
Marsch, E., Goertz, C. K., & Richter, K. 1982, J. Geophys. Res., 87, 5030
Marsch, E., Vocks, C., & Tu, C. Y. 2003, Nonlinear Process. Geophys., 10, 101
Matteini, L., Hellinger, P., Goldstein, B. E., et al. 2013, J. Geophys. Res.: Space Phys., 118, 2771
Mewaldt, R. A., Cohen, C. M. S., Haggerty, D. K., et al. 2003, Int. Cosm. Ray Conf., 6, 3313
Müller, D., Marsden, R. G., St. Cyr, O. C., & Gilbert, H. R. 2013, Sol. Phys., 285, 25
Müller, D., St. Cyr, O. C., Zouganelis, I., et al. 2020, A&A, 642, A1 (Solar Orbiter SI)
Nicolaou, G., Verscharen, D., Wicks, R. T., & Owen, C. J. 2019, ApJ, 886, 101
Owens, M. J., Crooker, N. U., & Schwadron, N. A. 2008, J. Geophys. Res.: Space Phys., 113, A11104
Owens, M. J., Lockwood, M., Riley, P., & Linker, J. 2017, J. Geophys. Res.: Space Phys., 122, 10,980
Paschmann, G., Fazakerley, A. N., & Schwartz, S. J. 1998, ISSI Sci. Rep. Ser., 1, 125
Pilipp, W. G., Miggenrieder, H., Mühlhaüser, K. H., et al. 1987, J. Geophys. Res., 92, 1103
Reinard, A. A., Lynch, B. J., & Mulligan, T. 2012, ApJ, 761, A175
Rodríguez-Pacheco, J., Wimmer-Schweingruber, R. F., Mason, G. M., et al. 2020, A&A, 642, A7 (Solar Orbiter SI)
Rouillard, A. P., Pinto, R. F., Vourlidas, A., et al. 2020, A&A, 642, A2 (Solar Orbiter SI)
Šafránková, J., Němeček, Z., Přech, L., et al. 2013, Space Sci. Rev., 175, 165
Šafránková, J., Němeček, Z., Němec, F., et al. 2019, ApJ, 870, 40
Schwadron, N., & McComas, D. 2003, ApJ, 599, 1395
Shearer, P., von Steiger, R., Raines, J. M., et al. 2014, ApJ, 789, 60
SPICE Consortium (Anderson, M., et al.) 2020, A&A, 642, A14 (Solar Orbiter SI)
Stansby, D., Perrone, D., Matteini, L., Horbury, T. S., & Salem, C. S. 2019, A&A, 623, L2
Steinberg, J. T., Gosling, J. T., Skoug, R. M., & Wiens, R. C. 2005, J. Geophys. Res.: Space Phys., 110, A06103
Tu, C., Zhou, C., Marsch, E., et al. 2005, Science, 308, 519
Velli, M., Harra, L. K., Vourlidas, A., et al. 2020, A&A, 642, A4 (Solar Orbiter SI)
Verscharen, D., Bourouaine, S., & Chandran, B. D. G. 2013, ApJ, 773, 163
Verscharen, D., Chandran, B. D. G., Bourouaine, S., & Hollweg, J. V. 2015, ApJ, 806, 157
Verscharen, D., Klein, K. G., & Maruca, B. A. 2019, Liv. Rev. Sol. Phys., 16, 5
von Steiger, R., Schwadron, N. A., Fisk, L. A., et al. 2000, J. Geophys. Res., 105, 27217
von Steiger, R., Zurbuchen, T., Geiss, J., et al. 2001, Space Sci. Rev., 97, 123
Walsh, A. P., Horbury, T. S., Owen, C. J., et al. 2020, A&A, 642, A5 (Solar Orbiter SI)
Wu, H., Verscharen, D., Wicks, R. T., et al. 2019, ApJ, 870, 106
Yoon, P. H., & Sarfraz, M. 2017, ApJ, 835, 246
Zhao, L., Zurbuchen, T. H., & Fisk, L. A. 2009, Geophys. Res. Lett., 36, L14104
Zouganelis, I., De Groof, A., Walsh, A. P., et al. 2020, A&A, 642, A3 (Solar Orbiter SI)
Zurbuchen, T. H. 2007, ARA&A, 45, 297
Zurbuchen, T., Hefti, S., Fisk, L., Gloeckler, G., & Von Steiger, R. 1999, Space Sci. Rev., 87, 353
Zurbuchen, T., Fisk, L., Gloeckler, G., & von Steiger, R. 2002, Geophys. Res. Lett., 29, A1352

[1] Mullard Space Science Laboratory, University College London, Holmbury St. Mary, Dorking, Surrey RH5 6NT, UK
e-mail: c.owen@ucl.ac.uk
[2] INAF-Istituto di Astrofisica e Planetologia Spaziali, Via Fosso del Cavaliere 100, 00133 Roma, Italy
[3] Southwest Research Institute, 6220 Culebra Road, San Antonio, TX 78238, USA
[4] Institut de Recherche en Astrophysique et Planétologie, 9, Avenue du Colonel ROCHE, BP 4346, 31028 Toulouse Cedex 4, France
[5] Laboratoire de Physique des Plasmas, Ecole Polytechnique, Palaiseau, France
[6] Centre National d'Etudes Spatiales, DCT/PO/EU – B.P.I. 2220, 18, Avenue Edouard Belin, 31401 Toulouse Cedex 9, France
[7] Techno System Developments S.R.L., Via Provinciale Pianura 2, Int. 23, San Martino Zona Industriale 80078, Pozzuoli, Italy
[8] NASA Goddard Space Flight Center, 8800 Greenbelt Road, Greenbelt, Maryland 20771, USA
[9] Planetek Italia S.R.L., Via Massaua, 12, 70132 Bari, BA, Italy
[10] Space Science Center, University of New Hampshire, Morse Hall, Durham, NH 03824, USA
[11] University of Michigan, 2455 Hayward St, Ann Arbor, MI 48109, USA
[12] LEONARDO, Viale del lavoro, 101, 74123 Taranto, Italy
[13] SITAEL S.p.A., Via San Sabino 21, 70042 Mola di Bari, BA, Italy
[14] ESA-ESTEC/SCI-PS, Keplerlaan 1, 2201 AZ Noordwijk, The Netherlands
[15] Department of Surface and Plasma Science, Faculty of Mathematics and Physics, Charles University, V Holesovickach 2, 18000 Prague 8, Czech Republic
[16] NASA Goddard Space Flight Center, 8800 Greenbelt Road, Greenbelt, MD 20771, USA
[17] CGC Instruments, Chemnitz, Germany
[18] Space and Atmospheric Physics, The Blackett Laboratory, Imperial College London, London SW7 2AZ, UK
[19] LESIA, Observatoire de Paris, Universite PSL, CNRS, Sorbonne Universite, Universite de Paris, 5 Place Jules Janssen, 92195 Meudon, France
[20] Space Research Group, University of Alcalá, 28801 Alcalá de Henares, Spain
[21] Agenzia Spaziale Italiana, Via del Politecnico, snc, 00133 Roma, Italy
[22] ESA-ESAC, Camino bajo del Castillo s/n, 28692 Villafranca del Castillo, Madrid, Spain
[23] Institute of Experimental and Applied Physics, Kiel University, Leibnizstrasse 11, 24118 Kiel, Germany
[24] Physikalisches Institut, Universitat Bern, Sidlerstrasse 5, 3012 Bern, Switzerland
[25] Incom, Inc., 242 Sturbridge Road, Charlton, MA 01507, USA